

DETC2017-68278

**MODULAR DESIGN OF A PASSIVE, LOW-COST PROSTHETIC KNEE MECHANISM
TO ENABLE ABLE-BODIED KINEMATICS FOR USERS WITH TRANSFEMORAL
AMPUTATION**

**Molly A. Berringer, Paige J. Boehmcke,
Jason Z. Fischman, Athena Y. Huang,
Youngjun Joh, and J. Cali Warner**
Massachusetts Institute of Technology
Cambridge, Massachusetts 02139
Email: mberring@mit.edu

V. N. Murthy Arelekatti
Global Engineering and Research Laboratory
Department of Mechanical Engineering
Massachusetts Institute of Technology
Cambridge, Massachusetts 02139
Email: murthya@mit.edu

Matthew J. Major
Department of Physical Medicine and Rehabilitation
Northwestern University
Chicago, Illinois 60611
Email: matthew-major@northwestern.edu

Amos G. Winter, V
Global Engineering and Research Laboratory
Department of Mechanical Engineering
Massachusetts Institute of Technology
Cambridge, Massachusetts 02139
Email: awinter@mit.edu

ABSTRACT

There is a significant need for low-cost, high-performance prosthetic knee technology for transfemoral amputees in India. Replicating able-bodied gait in amputees is biomechanically necessary to reduce the metabolic cost, and it is equally important to mitigate the socio-economic discrimination faced by amputees in developing countries due to their conspicuous gait deviations. This paper improves upon a previous study of a fully passive knee mechanism, addressing the issues identified in its user testing in India. This paper presents the design, analysis and bench-level testing of the three major functional modules of the new prosthetic knee architecture: (i) a four-bar latch mechanism for achieving stability during stance phase of walking, (ii) an early stance flexion module designed by implementing a fully adjustable mechanism, and (iii) a hydraulic rotary damping system for achieving smooth and reliable swing-phase control.

INTRODUCTION

Background and Motivation

This paper is a continuation of the work to design a fully passive prosthetic knee to enable able-bodied gait for transfemoral amputees in developing countries, based on a prior design and analysis by Narang, Arelekatti and Winter [1–5]. It is estimated that there are 200,000 above-knee amputees living in India and that 47% of amputees experience change or loss of employment following the amputation [6–8]. Severe social stigma and the economic consequences from having conspicuous disabilities have been well-documented and articulated [5, 9–13], highlighting the need for a low-cost prosthesis that can enable able-bodied gait to mitigate discrimination and increase metabolic efficiency.

Relevant Terminology

A brief summary of the relevant terms from gait biomechanics used in this paper are laid out briefly for the uninitiated reader (Fig. 1).

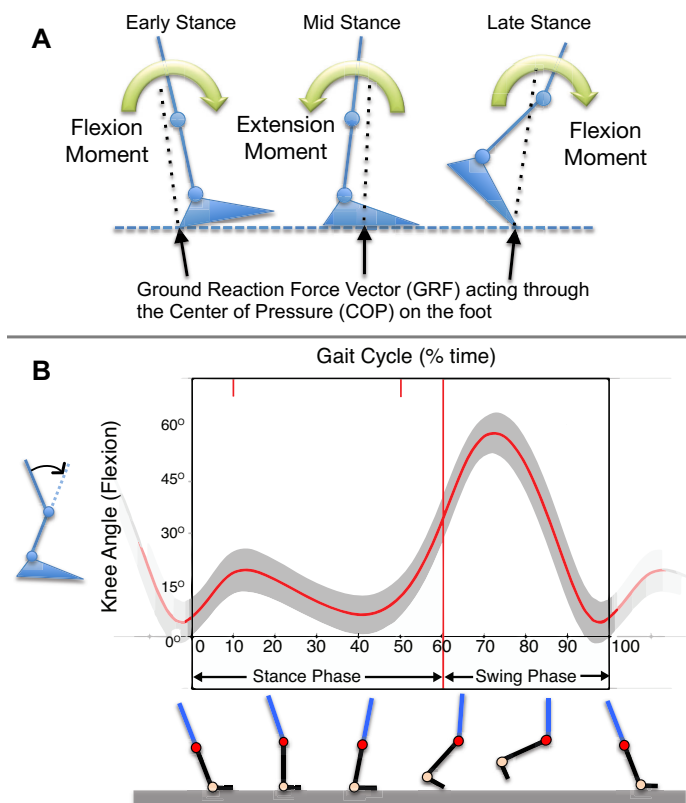


FIGURE 1: A. Illustration of the stance phase of gait cycle, when the foot is on the ground. The Ground Reaction Force (GRF) acting through the Center of Pressure (COP) results in flexion or extension moment through the stance phase. B. The human gait cycle of each leg is divided into the stance phase, followed by the swing phase when the foot leaves contact with the ground for clearance. The knee flexion angle is defined as the relative angle between the upper leg and lower leg as illustrated to the left of the vertical axis on the graph. Extension direction at the knee is defined to be in the opposite direction to the flexion direction. The graph shows the normative knee angle kinematics through the gait cycle (red curve), along with the standard deviation shown in grey band [14]. The illustration below the horizontal axis shows the corresponding lower leg trajectory through the gait cycle

Existing Devices and their Limitations

A significant cost-performance gap exists in the realm of current knee prostheses. Advanced, high-performance prosthetic devices used in the developed world are typically active in order to achieve optimal performance, making them inappropriate for the developing world in terms of cost as well as sub-optimal for large-scale, resource-constrained application [5, 15, 16]. Typical developing world prostheses are passive and low-cost, but primitive in functionality, inhibiting able-bodied gait and garnering poor user satisfaction [12, 15]. Manually locked knees are cur-

rently the most widely distributed prosthetic knees in developing countries. The four-bar polycentric four-bar knee is currently being adopted in India and other countries, and shows better performance than previous single-axis joints [12]. While similar knees have shown better performance than the locked or single-axis devices, they notably fail to address early stance flexion or proper timing in later flexion [5]. The LCKnee designed by Andrysek et al. [17, 18] with a reliable single-axis mechanical latch addresses complaints of falling due to buckling in other devices. However, early stance flexion and late phase damping required for able-bodied kinematics [5] have not been satisfactorily addressed. Recent work by Arelekatti and Winter [3, 5] is moving towards the development of a low-cost passive prosthetic knee, addressing these outstanding needs and allowing for an efficient walking gait. By modeling knee angle, moment, and power over the course of a gait cycle, it was determined that a close approximation of healthy knee function could be achieved passively using a spring activated at early stance, and two dampers activated over the course of the late stance and swing phases [1, 2]. This analysis was used to develop low-cost, passive, prosthesis prototypes [3–5] with an automatic stance phase lock for stability. The prototypes were tested on four above-knee amputees in India. The desired early-stance flexion was not observed in amputee gaits, despite incorporating the necessary elastic module. Additionally, these prototypes relied on zero order dampers (using friction brakes) and friction-based automatic latch for stability during early stance. This reliance on friction made the prototype unsuitable for long term use [5].

Three Modules: Stance Stability, Early Stance Flexion and Swing Control

This paper presents improvements that address the main deficits identified in the earlier prototypes. This iteration of the design was approached with the aim to deterministically enable the desired gait kinematics, working specifically on the three modules identified to be problematic in the previous device: stance stability, early stance flexion, and swing-phase control. This paper is divided into modules to describe the design and analysis for each module, given the basic operation and architecture of the overall device has been discussed in the published literature [1–5]. Results are discussed together for the first two modules and separately for the third module.

MODULE 1: STANCE STABILITY

Overview and Strategy

Stance stability is a critical function of the knee prosthesis as it is directly related to the user's safety. The main design requirements for this module are the ability to withstand a flexion moment of 40Nm (caused by GRF) without buckling, allow quick transition into the swing phase, ensure the mechanism is

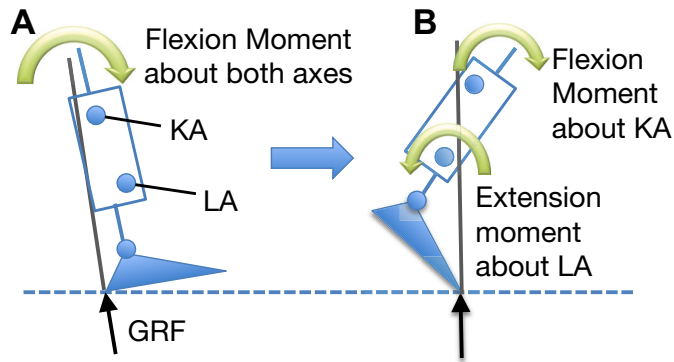


FIGURE 2: A. In early stance, the ground reaction force causes flexion moments about both the knee axis (KA) and locking axis (LA). B. In late stance, the ground reaction force causes a flexion moment about the knee axis but an extension moment about the locking axis.

latched before heel strike, and reduce backlash in the mechanism to prevent hyperextension (to within 1°) [7]. Hyperextension is the knee extending backwards from the neutral standing position. Various locking and braking mechanisms for single and multiple axis knees were considered, before it was decided to focus on implementing a single-axis, automatically locking mechanism [17]. This strategy was chosen for its absolute stability, simplicity, and durability.

In an able-bodied gait cycle, the knee experiences a flexion moment during both the early and late phases of stance (Fig. 1). In early stance, the knee must stay locked to prevent buckling, while in late stance the knee should be unlocked to initiate swing. An innovative solution is to use a latch mounted on a locking axis to control the engagement of a latch [15]. By carefully placing this locking axis with respect to the ground reaction force and knee axis, the locking axis can experience a flexion moment in early stance and an extension moment in the late stance (Fig. 2). The different moments can be used to engage and disengage the latch. Similar to the latch design by Andrysek [17], this strategy was implemented in Arelekatti and Winter's previous design [3–5] with some success, and a key improvement to its performance has been made by switching from using a physical locking axis to a virtual axis. The four-bar implementation of this virtual axis is discussed in more detail in the next section.

Design and Analysis

Mechanism Design A sectional view of the stance stability module at key points during the gait cycle is shown in Fig. 3. The main components of the design include: (i) the knee piece, which is connected to the early stance flexion module and the socket and rotates with respect to the knee axis, (ii) the latch piece, which extends to the base and connects to the lower pylon,

and (iii) the linkages of the four-bar mechanism that create a virtual locking axis. There are also two pieces that act as hard stops and limit the rotational motion of the knee and latch (Fig. 3 circular inset). The latching mechanism involves four major steps, the first two occurring during stance phase and the latter two occurring during swing phase:

1. Locked position (Fig. 3A) - when the user's heel first strikes the ground, the knee experiences a flexion moment, but the latch is in the locked position and flexion is prevented by the mechanical engagement of the knee with the latch tip.
2. Latch unlocking (Fig. 3B) - as the user rolls over on the foot and the GRF moves towards the toes and in front of the knee axis, the knee experiences an extension moment which disengages it from the latch tip and also presses the knee against a hard stop. This allows the latch to move freely backwards against the spring when the GRF passes in front of the locking axis. With the latch now in the unlocked position, the knee is allowed to rotate under a flexion moment as the GRF passes back behind the knee axis (Fig. 2).
3. Latch repositioning (Fig. 3C) - once the knee has flexed and swing initiated, the restoring bias-spring force will return the latch to the locked position.
4. Latch relocking (Fig. 3D) - as the lower leg and foot swing forward to extend at the end of the gait cycle, the knee will come down on the latch tip, pushing it back against the spring until the knee has extended far enough to allow the restoring spring force to relock the knee.

Note that in the relocking step (Fig. 3 circular inset), there is a unique feature in the knee piece that allows for relocking at two different points, which is referred to as a double latch. This allows the knee to lock at an intermediate point before reaching full extension (currently designed to be at 10° of knee flexion). This is important for user's safety because it means the knee will lock even if the user does not fully extend the knee before heel strike, as may happen when walking up inclines.

Placement of the Locking Axis In a normal gait cycle, the center of pressure (COP) of the GRF moves from the heel to the toe [14] (Fig. 4). This means the GRF's orientation in space can be deterministically used to unlock the latch at a desired instance in the gait cycle. As the GRF passes a certain point, the latch switches from being engaged to disengaged, allowing the knee to swing. This GRF transition point is determined by the projection down to the foot of the line that connects the knee axis and the locking axis. So by determining a desired GRF transition point, the placement of the locking axis can be limited to the line connecting the GRF transition point and the knee axis (Fig. 4). In order to imitate an able-bodied gait cycle, it was decided that the GRF transition point should be placed at the COP when the knee initiates late stance flexion, as shown in Fig. 4. From Win-

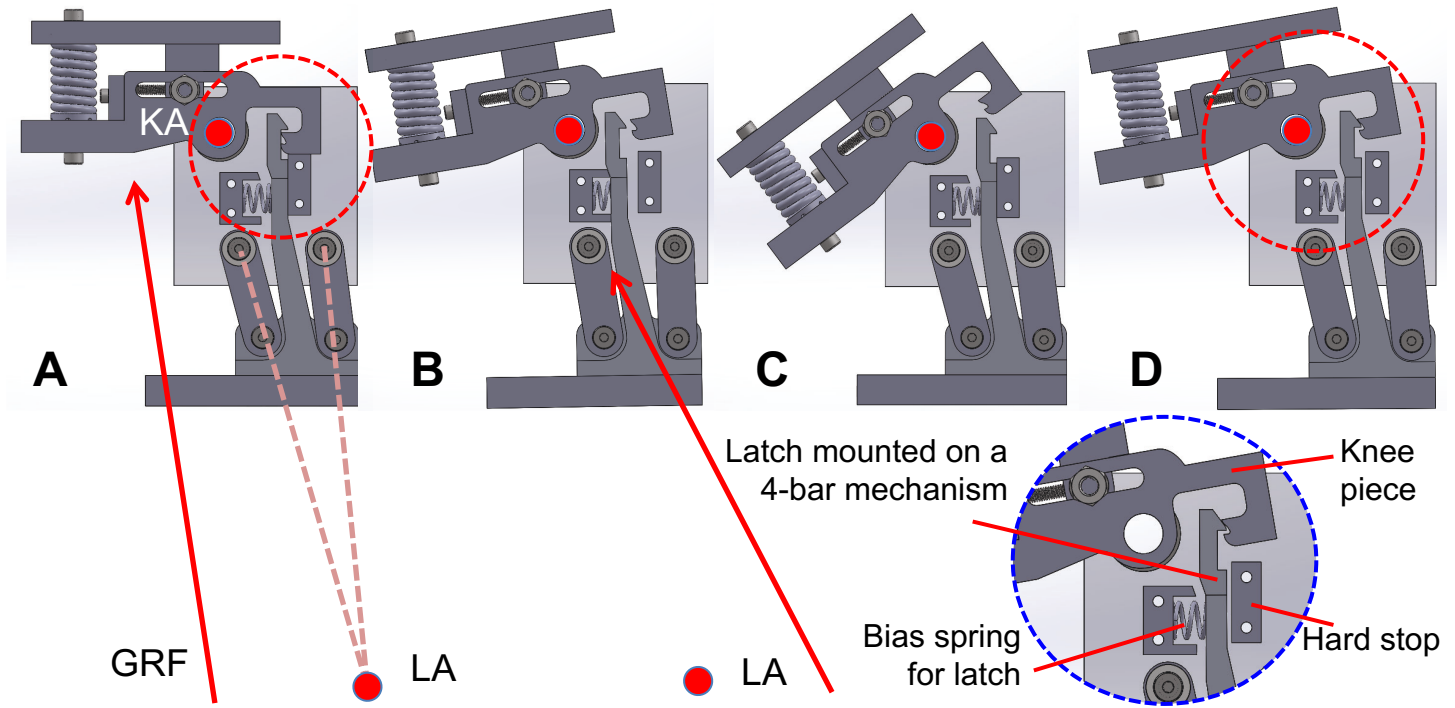


FIGURE 3: The stance stability module at (from left to right): A. locked position, B. latch unlocking, C. latch repositioning, and D. latch relocking. The red line represents the ground reaction force and the red dots are the knee axis and the virtual locking axis (KA and LA respectively). The circular inset shows the different parts important in the function of the stability module. The step by step function of the module is described in detail in the section on Mechanism Design.

ter's gait data [14], it was that decided the GRF transition point should be 18 cm from the heel [14].

After deciding upon the GRF transition point to constrain the locking axis to a line, the height and exact placement of the locking axis was determined to reduce hyperextension while maintaining stance stability. Hyperextension results in a small wobble the user feels as the latch unlocks during mid stance extension. The relationship between the hyperextension angle and latch unlocking movement can be modeled by a simple angle-arc length relationship:

$$s = r\theta \quad (1)$$

where s is the latch movement when it unlocks, r is the vertical distance between the knee axis and the locking axis (Fig. 4), and θ is the hyperextension angle at the knee. Users were able to distinctly notice hyperextension in the earlier knee design [3–5], which had approximately 3° of hyperextension. Less than 1° of hyperextension is desired. The latch movement was measured to be 5 mm. Therefore, to achieve the goal of reduced hyperextension, the locking axis was designed to be 30 cm below the knee axis. However, while a low locking axis can reduce hyperextension,

it also means that a wider range of GRFs will be able to unlock the knee.

The locking axis can be implemented in two ways: a physical axis or a virtual axis using a four-bar mechanism. Whereas the physical axis uses fewer parts and is more robust (implemented in the LCKnee by Andrysek [17]), the virtual axis allows much more flexibility in placing the locking axis and can result in a more compact design. Since the desired location of the locking axis is far apart from the knee axis, a virtual implementation was chosen as a physical, single-axis implementation of the locking member (latch) would have been too bulky.

Structural Analysis of the Latching Mechanism

The structural integrity of the latching mechanism at heel strike is critical to keep the knee locked and prevent buckling. A free body diagram of the relevant forces on the system at heel strike is shown in Fig. 5. The sum of moments on the latch about the locking axis, ΣM_{LA} is:

$$\Sigma M_{LA} = GRF \cdot d_{GRF} + f_{spring} \cdot d_{spring} + f \cdot d_f + N \cdot d_n - f_{hs} \cdot d_{hs} \quad (2)$$

where d_{GRF} , d_{spring} , d_f , d_n and d_{hs} are the lever arm dis-

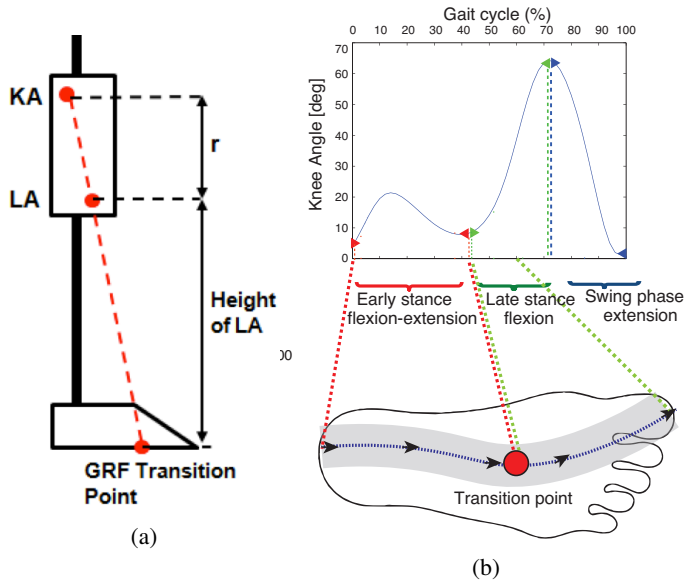


FIGURE 4: A. Placement of the locking axis along the line between the knee axis and GRF transition point. B. Movement of COP during a gait cycle, mapped to the corresponding knee angle kinematics. The placement of GRF transition point is at the beginning of late stance flexion of the knee.

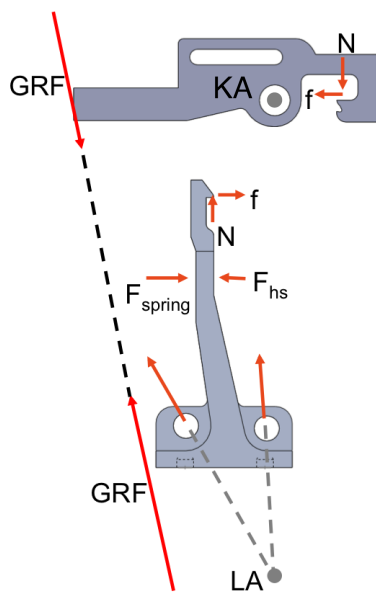


FIGURE 5: Free body diagram of the knee and latch at heel strike.

tances from the knee axis of the respective forces (Fig. 5). All forces on the latch create a positive moment that helps to keep it in the locked position, other than the reaction force from the hard

stop the latch presses against. This means that the only reason the latch might unlock at this stage is structural failure at the tip, but beam bending and tensile strength calculations show that the latch tip can withstand the applied normal forces. To increase the factor of safety, the latch tip will be machined from the stronger Aluminum 7075, while the rest of the parts can be machined from the more common Aluminum 6061 alloy (or injection molded in plastic in future iterations). This analysis suggests that this design provides robust locking and will successfully mitigate the risk of buckling at heel strike.

It is a key point that this stance stability mechanism relies on mechanical engagement to keep the knee locked. This addresses the main drawback of Arelekatti and Winter's previous design [3–5], which relied on friction between the knee and latch pieces to keep the knee locked. Any issues with the unreliability or variability of friction forces, or with the knee unlocking under forces high enough to overcome friction, are no longer seen in the current design.

MODULE 2: EARLY STANCE FLEXION

Overview and Strategy

The development of an early stance flexion (ESF) module was one of the three main focuses of the design of this prosthesis. While prostheses designed for the developing world ignore early stance flexion, it is critical that it be accommodated to a magnitude of 20 degrees to replicate able-bodied kinematics during the early stance phase of walking gait (shown in Fig. 1B, the ~20 degree bump in the knee angle curve). The lack of early stance flexion is detrimental to the user because of both the social stigma associated with the conspicuous gait deviation, as well as the potential long term health issues of lacking cushioning provided after heel strike, and having to compensate for lack of such flexion through over-exertion at the the hip. This design aims to build off of the previous work by Narang, Arelekatti and Winter, improving the design and increasing its adjustability to try to achieve early stance flexion in future user trials. While the previous design had implemented ideal parameters calculated through biomechanical analysis, this one aims to allow for a wider range of adjustment in order to experimentally determine the proper parameters that will be necessary in order to ensure early stance flexion in the future devices.

The previously developed prosthesis determined the positioning and stiffness for the early stance flexion axis of rotation by looking at the changing ground reaction force (GRF) vector of an able-bodied subject over the gait cycle. Since the GRF changes direction over the gait cycle, it is possible to position a rotational axis such that the axis is torqued in one direction by the GRF at one point in time, and torqued in the opposite direction at a later time in the gait cycle. In order to accurately determine the proper position to locate this axis in order to get the desired transition point, the GRF profile must be accurately

known. However, one of the largest sources of uncertainty in this process is the GRF profile of a transfemoral amputee during testing. Particularly, because of variation among users in choice of prosthetic feet, previous prosthetic knee experience, and general experience using a prosthetic limb, it is expected that different users will have developed their own slightly different GRF profiles. These forms of variability in the GRF profiles make it difficult to determine the appropriate knee parameters such as joint stiffness and axis placement prior to testing. This uncertainty motivates the focus on maximizing the adjustability of this module.

There were three main factors of adjustability incorporated into this design. The first was the ability to change the effective torsional stiffness in order to make it easier or harder for the knee to flex. The second was the ability to preload the spring within the ESF module, in order to both eliminate backlash and determine the minimum desired force for flexion. Finally, the third was the ability to change the location of the axis of rotation, in order to account for varying GRF profiles from transfemoral amputee users.

Design and Analysis

Changing Effective Torsional Stiffness The torsional stiffness of the axis is created by having a simple compression spring connected to the module at a distance D from the axis of rotation (Fig. 6A, 6C). When the knee attempts to flex, the spring is compressed (Fig. 6B), and when the knee is locked for stance stability, the spring hits a hard stop and to prevent hyperextension. The torsional stiffness is therefore directly related to both the spring stiffness, K , and the distance, D . The design incorporates a large slot such that D can be changed within the range of 2.4 cm to 5.4 cm. This allows the doubling of the moment arm and a commensurate increase in the effective stiffness about the ESF axis. Additionally, the design allows for the easy replacement of different springs into the module. By allowing for the substitution of multiple varying springs into the module for testing, it is possible to vary the K value and cover a wide range of effective axial stiffnesses. By combining these two techniques, the design is capable of achieving a coarse adjustment through its stiffness, and a fine adjustment through its moment arm. Based on the range of compression springs sourced, the design was capable of reaching torsional stiffness in the range of 0.8 – 7.0 Nm/kg – rad, well encompassing and going beyond the calculated ideal stiffness for this axis by Narang and Winter (2.96 Nm/kg – rad [1]).

Spring Preload The preload is applied by the use of a wide nut with a conical surface for the spring to rest on (Fig. 6C). By rotating the nut on its base screw, the nut can be moved upwards in order to preload the spring. This preload works to eliminate backlash that would otherwise be inherent within the design

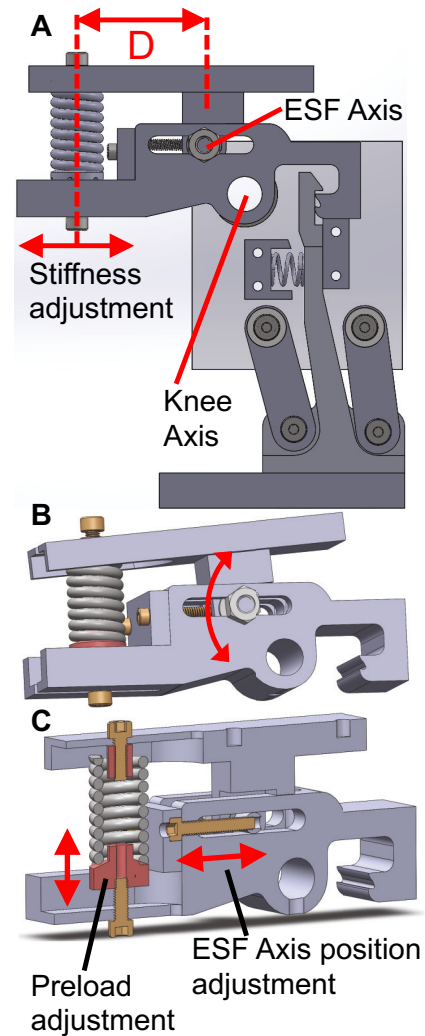


FIGURE 6: A. Knee assembly cross section: stiffness adjustment in the early stance flexion module by lateral movement of the spring. The spring slot was changed to be open on the ends for easier loading and unloading of springs. Note the distance, D , between the spring and the ESF axis. B. ESF module flexion shown about the ESF axis. C. Sectional view: axle nuts on the ends of ESF axis to hold the module in place in the slot, as well as a preload device on the bottom of the spring.

and was reported to be uncomfortable in the past trials [5]. Additionally, by preloading the spring, the tester can set a specific threshold torque that must be applied to the knee before it will overcome the preload and begin to flex in early stance. This is important because if the users begin to feel flexion at the beginning of early stance, they may suspect that the knee is buckling and will be overtly cautious to apply their proper weight to it. However, if the spring is preloaded, flexion would not be felt

immediately, and could only become apparent once the user is applying the proper weight to the prosthesis.

Changing Position of the Early Stance Flexion Axis

The design of the ESF module that is flexed and released at different points in the gait cycle is reliant on the GRF vector eventually passing from one side of the ESF axis of rotation, to the other. When testing with users that have potentially varying GRF profiles, such as transfemoral amputees, it is important that the design be adaptable in its ESF axis location. This adaptability is achieved using a set of axle nuts as well as a lead screw mechanism (Fig. 6B,C). The axis itself is a steel rod with a threaded hole down its center, and an 8-32 screw passing perpendicularly through it. This screw is held in place by an end cap, such that when it is turned, the axis will be moved backwards and forwards, as in a lead screw mechanism. Once a desired location for the axle is found, a nut is tightened down on either side of the axle, in order to ensure that it does not slip from the desired location. The length of this adjustability is 3.2cm. The farthest anterior that the axis may be moved is such that it is in line with the knee axis. It would be undesirable to begin moving the axis further anterior to this point, because it would then become likely that the axis would be constantly torqued in flexion and the GRF would never pass anterior to it in order to release the spring and allow straightening of the knee.

RESULTS: MODULE 1 AND MODULE 2

Module 1: Stance Stability



FIGURE 7: Testing the knee prototype with a knee simulator, showing both the latch and the early stance flexion modules.

After design and analysis of the two modules, the metal parts for both the latch and the early stance flexion modules were CNC machined and assembled at MIT. A pylon and a passive pros-

thetic foot (Jaipur foot [19, 20]) were attached to the lower leg, and the knee top was attached to a knee simulator, to allow us to test the knee (Fig. 7).

Three authors of the paper used the knee simulator to qualitatively test the knee. Testers were able to walk normally without the knee buckling or failing to unlock. One tester was also able to walk with the knee at both slow and normal speeds across the length of MIT's Killian Court without issues. Qualitative feedback showed that testers felt stable on the knee, and trusted putting their body weight on it more than during previous tests of the 4-bar prosthetic knee [5, 16].

Prior to testing on the ground, the locking mechanism for stance stability was tested by hand by rolling over the foot to simulate the loads applied during a gait cycle. Various stiffness bias springs were tested (Fig. 3 inset), and it was observed that a bias spring with a stiffness constant greater than the calculated, allowable range resulted in an inability to unlock the knee. On the other hand, for a spring with a spring constant less than the allowable range, the knee would not reliably relock. This proved that the calculated range of spring constants was reasonable. Overall, a latching mechanism to provide stance stability was designed, prototyped, and tested. Stance stability was emphasized as the most critical function of the knee prosthesis, and user testing and feedback showed that the prototype performed well, in terms of stance stability.

Future work includes testing the latching mechanism on inclines or uneven terrain. The prototype knee was tested only on flat surfaces, but the design and analysis suggest that the knee can function well on inclines, as the locking axis placement can be chosen such that the expected GRFs will unlock the knee at the appropriate time. The double latch's intermediate locking point allows the knee to lock before reaching full extension, which is particularly advantageous for walking uphill.

Module 2: Early Stance Flexion

While the prosthesis must still be validated in user trials, this prototype was capable of covering a very broad range of functional parameters for achieving early stance flexion. Using springs with a stiffness of up to 175 N/mm, the axial stiffness possible exceeded 7 Nm/kg – rad, whereas the previously calculated ideal was 2.96 Nm/kg – rad. Additionally, the axis of rotation was capable of being shifted by up to 3.2cm, and the maximum deflection achievable was over 22°. These parameters are dependent highly on the specific springs used during testing, but because of the modularity of the system and the ability to easily replace springs, the ESF module will be capable of covering very broad ranges of stiffness, axial placement, and preload.

MODULE 3: SWING-PHASE CONTROL

Overview and Strategy

The last critical module is the swing-phase control, which controls the motion of the leg during late-stance flexion and swing-phase flexion and extension (Fig. 1B). Narang [1], in previous work, identified the need for a damping system during the late-stance phase and the swing phase, since negative work is performed during these two phases of the gait cycle. Narang also developed a model, based on the weight distribution of prostheses for transfemoral amputees, that identifies the moment needed about the knee axis over the gait cycle, thus allowing him to identify a disparity in the amount of damping needed between flexion (during late stance and early swing) and extension (during late swing): approximately four times as much damping is needed during flexion compared to swing phase extension at normal gait speed [1]. Previous work by Arelekatti and Winter [3, 5] used this information to create a low-cost damping system that included two dampers with friction pads with a one-way clutch. This allowed both friction dampers, the larger and the smaller, to be engaged during flexion, while only the smaller was engaged during extension [5].

Although the use friction pads by Arelekatti and Winter in the earlier prototype was consistent with the findings of Narang [1], relying on friction pads fails to meet the requirement for robustness and durability as they are susceptible to wear over time and are subject to environmental elements like water and dust. More importantly, friction-based damping exhibited stick slip phenomenon, i.e. a non-zero torque was required to initiate motion to overcome the static friction. This was reported to be undesirable by all the users in past trials [5]. Additionally, friction pads offered only a constant damping value, failing to accommodate changes in gait speed [1]. The task for this module was to improve upon the Arelekatti and Winter damping system by addressing these drawbacks while keeping the system low cost and robust.

Many damping alternatives to friction pad dampers were investigated. Pneumatic and hydraulic systems were considered for first and second order damping. Size limitations make pneumatic systems impractical choices for damping because of relatively high compressibility of air. Therefore, the new design considered two hydraulic based designs: a linear hydraulic damper and a rotary hydraulic damper.

Design and Analysis

Optimization analysis of different damping systems Two initial damping models were created (Fig. 8). The first included a linear hydraulic damper in a slider-crank arrangement (Fig. 8A): the piston's revolute joint connected to the rotating knee part on the upper leg and the bottom revolute joint was fixed to the lower leg. This linear damper model assumed bi-directional damping within the linear damper due to one-

way valves in the piston head. The other model was two rotary dampers connected on either side of the knee axis, mounted coaxially on one-way roller clutch bearings (Fig. 8B). Similar to the previous design with friction pad dampers, this would allow for one rotary damper to be engaged during flexion and the other engaged during extension.

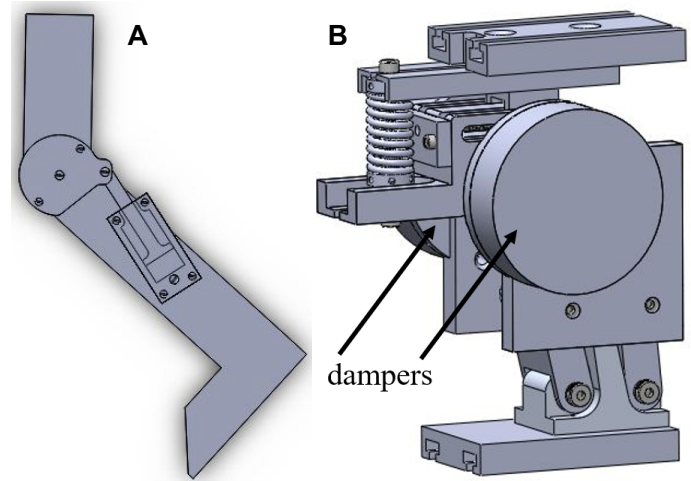


FIGURE 8: A. Two-dimensional model of linear damper connection geometry. B. Three-dimensional model of rotary dampers incorporated into the final design

A MATLAB script was created to analyze how well these new damping systems and the previous friction pad damping system matched the knee moment curve modeled by Narang [1, 2], using the able-bodied gait biomechanics including knee angle and knee angular velocity [14]. From 0 to 40 percent of the gait cycle, i.e. during early stance phase (Fig. 1B), the ideal spring for ESF identified by Narang, was used [1]. From 40 to 100 percent of the gait cycle (Fig. 1B), the damping systems would be engaged on the prosthesis.

In the friction damping system, the moment, M , is a constant value during flexion and a different constant value during extension, due to the differential damping system with friction pad dampers mounted on one-way roller clutch bearings [5].

For a linear viscous damper, the moment, M , created from the linear damper with piston velocity, v , and damping coefficient, b_l , is:

$$M = -b_l v^2 \quad (3)$$

The rotary damper design depends on a very viscous fluid between two rotating components and therefore depends on the angular velocity ω . The moment, M , created from the hydraulic

rotary damper with angular velocity, ω , and rotary damping coefficient, b_r , is the product of the damping coefficient and the angular velocity:

$$M = -b_r \omega \quad (4)$$

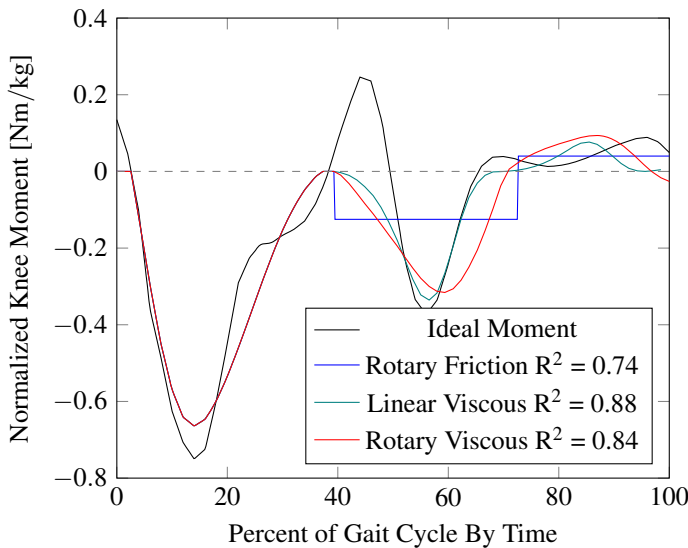


FIGURE 9: Ideal knee moment curve for a knee prosthesis as modeled by Narang [1]. An ideal ESF spring is incorporated between 0 and 40 percent of the gait cycle and different damping systems of this study engaged from 40 to 100 percent of the gait cycle.

The results of the model optimization are shown in Fig. 9. The correlation between the ideal moment profile and the moment profiles from these different damping systems was found by calculating R^2 (coefficient of determination) values. The R^2 values were 0.74, 0.88, and 0.84 for the friction pad dampers, linear hydraulic damper, and the hydraulic rotary dampers, respectively. The R^2 values of the two hydraulic damping systems were both greater than the R^2 value for the friction pad dampers, showing either would be an improvement to the previous design. Although the R^2 value of the linear hydraulic damper was greater than that of the rotary implementation, both designs were considered, and the benefits and drawbacks of each were analyzed. The rotary damper system was eventually chosen because of the advantages of simple integration, less leakage due to the dynamic seal being a rotating one rather than a sliding one, and the simple design of the damper which does not need an accumulator or orifices as would be required in a linear damper.

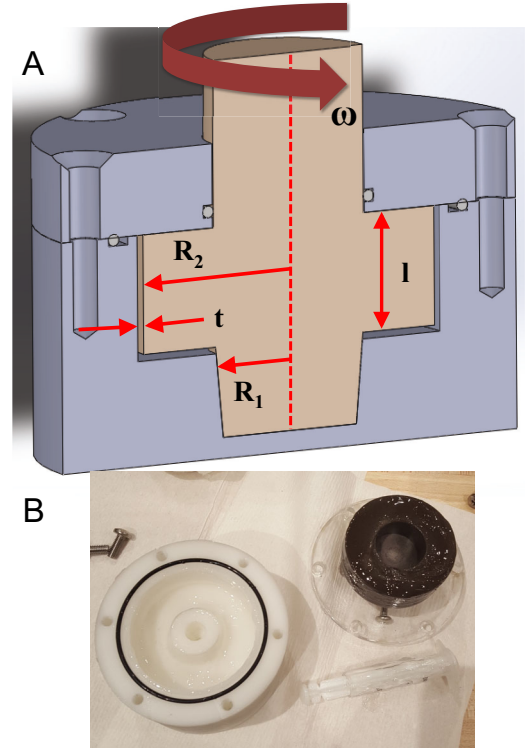


FIGURE 10: A. Rotary damper prototype showing the plunger (tan) and the cylindrical chamber (gray); the relevant parameters are related in equation 5. B. Photograph of the disassembled damper showing chamber (white) with O-ring and plunger (black).

Rotary damping A prototype of the rotary damper was constructed in three parts (Fig. 10). First, a cylindrical chamber was milled from Delrin. Next, a plunger was turned and milled from Teflon-infused Delrin (for low friction) and inserted into the chamber. Finally, an acrylic lid was laser-cut to size and screwed on top of the device. A rubber O-ring was used between the cylindrical chamber and the acrylic lid to prevent leaking, and a small spring was used to hold this rotating plunger tight against the lid. The plunger rotates inside the stationary cylindrical chamber, exerting a force on the viscous fluid inside the chamber that causes the damping torque.

The rotary damper prototype is governed by the following analytical relationship:

$$B_{viscous} = \frac{T}{\omega} = \frac{\pi\mu}{t} \left(2lR_2^3 + \left(\frac{R_2^4}{2} - \frac{R_1^4}{2} \right) \right) \quad (5)$$

where $B_{viscous}$ is the rotary damping coefficient, T is the damping torque, ω is rotational velocity, μ is liquid viscosity.

Parameters R_2 , R_3 , l , and t are labeled in Fig. 10. This relationship was arrived at by summing up the viscous torque exerted by the relative rotation of concentric cylinders in a viscous medium and the torque due to the annular plate rotating on top a fixed flat plate with a viscous medium in between [21].

The damper was assembled and tested with pure Silicone oil (kinematic viscosity $1.0\text{m}^2/\text{s}$), because it is one of the highest viscosity fluids available, and it is commonly used in hydraulic dampers of similar design. Using a flexural torque wrench, the torque required to rotate the damper 180° in a given time was measured. Thus, the outputs of this experimental test were torque and angular velocity, which were compared to the expected torque value from Equation (5) on the preceding page. The viscous material has a crucial impact on the amount of damping this prototype could achieve.

RESULTS: MODULE 3

The torque values measured for the rotary damper prototype were in the range of 3Nm – 5Nm at moderate angular velocities between 3.14 and 6.28rad/s (30 rpm to 60 rpm , common range for walking gait), compared to the expected range of 2.67Nm and 3.04Nm , respectively (Equation (5) on the previous page). Due to the shear thinning properties of silicone oil, the torque does not increase linearly with angular velocity. This is a necessary consideration in future iterations of the damper in order to determine proper scaling relationships. Another consideration is that the maximum damping force required to match able-bodied kinematics is up to 21Nm at moderate angular velocities. Based on Equation (5) on the preceding page, increased torque can be achieved by increasing the number of concentric circular walls and by decreasing the gap between the walls, as is available in some commercial dampers.

Having validated the feasibility of the concept, the final device will utilize two rotary dampers mounted on the knee axis, one engaged on a one-way roller clutch bearing to provide damping in flexion, and the other engaged on an opposite one-way clutch to provide the damping required during extension.

DISCUSSION AND CONCLUSION

Given the pressing social and physiological need for high performance, low-cost prosthetic devices in the developing world, greater research in the field of low-cost passive prostheses is critical. This paper describes a new analytical and mechanical approach through which to realize the theoretical prosthesis presented in the past work in the literature [1, 3, 5]. Through various deterministic design changes within the mechanisms of the prosthesis, a passive knee was designed with the goal of enabling able-bodied gait and higher metabolic efficiency in transfemoral amputees.

A working ESF module was designed with the goal of enabling able-bodied gait during stance; a latch to ensure complete stance stability; the fluid dampers to ensure reliable swing-phase control. All three modules together have been designed to work together to enable able-bodied gait over the entire gait cycle. The initial bench level testing that was performed showed promising results. Rotary dampers of the correct torque values still need to be prototyped and then added to the prosthetic knee. Patient testing is also needed to qualitatively validate the current approach. Future iterations of the prototype are slated to be tested on experienced subjects, both in India and the US. Once the operation of the device has been validated in the field, the prosthesis will be redesigned for manufacture at scale, with increased focus on meeting the cost and aesthetic design requirements.

ACKNOWLEDGMENT

Infinite gratitude to Matthew Cavuto and GEAR Lab for their help to guide this project through ideas, feedback, and resources. Additional thanks to project partners Professor Matthew Major at Northwestern University and Dr. Pooja Mukul at Bhagwan Mahaveer Viklang Sahayata Samiti (BMVSS) for their feedback and guidance. The work was carried out as part of “2.76: Global Engineering” graduate design class taught by Prof. Amos G. Winter at MIT Mechanical Engineering.

REFERENCES

- [1] Narang, Y. S., Arelekatti, V. M., and Winter, A. G., 2016. “The effects of the inertial properties of above-knee prostheses on optimal stiffness, damping, and engagement parameters of passive prosthetic knees”. *Journal of Biomechanical Engineering*, **138**(12), p. 121002.
- [2] Narang, Y. S., Arelekatti, V. M., and Winter, A. G., 2016. “The effects of prosthesis inertial properties on prosthetic knee moment and hip energetics required to achieve able-bodied kinematics”. *IEEE Transactions on Neural Systems and Rehabilitation Engineering*, **24**(7), pp. 754–763.
- [3] Arelekatti, V. N. M., and Winter V, A. G., 2016. “Design of a fully passive prosthetic knee mechanism for transfemoral amputees in india”. *Journal of Mechanisms and Robotics*. In Press.
- [4] Arelekatti, V. M., and Winter, A. G., 2015. “Design of mechanism and preliminary field validation of low-cost, passive prosthetic knee for users with transfemoral amputation in india”. In ASME 2015 International Design Engineering Technical Conferences and Computers and Information in Engineering Conference, American Society of Mechanical Engineers, pp. V05AT08A043–V05AT08A043.
- [5] Arelekatti, V. M., and Winter, A. G., 2015. “Design of a fully passive prosthetic knee mechanism for transfemoral

- amputees in india". In Rehabilitation Robotics (ICORR), 2015 IEEE International Conference on, IEEE, pp. 350–356.
- [6] Narang, I. C., Mathur, B. P., Singh, P., and Jape, V. S., 1984. "Functional capabilities of lower limb amputees". *Prosthetics and Orthotics International*, 8(1), Apr., pp. 43–51.
- [7] Narang, Y. S., 2013. "Identification of Design Requirements for a High-Performance, Low-Cost, Passive Prosthetic Knee Through User Analysis and Dynamic Simulation". Master's thesis, Massachusetts Institute of Technology, Cambridge MA, May.
- [8] Narang, Y., Austin-Breneman, J., Arelekatti, V. N. M., and Winter, A., 2016. "Using biomechanical and human-centered analysis to determine design requirements for a prosthetic knee for use in India". *In review*.
- [9] Rybarczyk, B., Nyenhuis, D. L., Nicholas, J. J., Cash, S. M., and Kaiser, J., 1995. "Body image, perceived social stigma, and the prediction of psychosocial adjustment to leg amputation". *Rehabilitation Psychology*, 40(2), p. 95.
- [10] Horgan, O., and MacLachlan, M., 2004. "Psychosocial adjustment to lower-limb amputation: a review". *Disability and Rehabilitation*, 26(14-15), pp. 837–850.
- [11] Mohan, D., 1967. "A Report on Amputees in India".
- [12] Hamner, S. R., Narayan, V. G., and Donaldson, K. M., 2013. "Designing for Scale: Development of the ReMotion Knee for Global Emerging Markets". *Annals of Biomedical Engineering*, 41(9), Sept., pp. 1851–9.
- [13] Wyss, D., Lindsay, S., Cleghorn, W. L., and Andrysek, J., 2013. "Priorities in lower limb prosthetic service delivery based on an international survey of prosthetists in low- and high-income countries.". *Prosthetics and orthotics international*, Dec.
- [14] Winter, D. A., 2009. *Biomechanics and Motor Control of Human Movement*, 4th ed. John Wiley & Sons, Inc.
- [15] Andrysek, J., 2010. "Lower-limb prosthetic technologies in the developing world: a review of literature from 1994-2010". *Prosthetics and Orthotics International*, 34(4), pp. 378–398.
- [16] Hamner, S. R., Narayan, V. G., and Donaldson, K. M., 2013. "Designing for Scale: Development of the ReMotion Knee for Global Emerging Markets". *Annals of Biomedical Engineering*, 41(9), Sept., pp. 1851–9.
- [17] Andrysek, J., Klejman, S., Torres-Moreno, R., Heim, W., Steinnagel, B., and Glasford, S., 2011. "Mobility function of a prosthetic knee joint with an automatic stance phase lock". *Prosthetics and Orthotics International*, 35(2), pp. 163–70.
- [18] Wyss, D., 2012. "Evaluation and design of a globally applicable rear-locking prosthetic knee mechanism". PhD thesis, University of Toronto.
- [19] Bhagwan Mahaveer Viklang Sahayata Samiti, 2014. What We Do: Above Knee Prosthesis. <http://jaipurfoot.org/> (Accessed 5/19/14).
- [20] Sharp, M., 1994. "The Jaipur limb and foot". *MEDICINE AND WAR*, 10, pp. 207–211.
- [21] Kundu, P. K., Cohen, I. M., and Dowling, D. R., 2015. *Fluid Mechanics*. Academic Press.